

Instrumentation for Particle Physics – in four lectures

Lecture III: Tracking and Calorimetry

Sally Seidel
University of New Mexico

African School of Physics 2021

Tracking Detectors:
Measure particle trajectory (curvature, momentum)
and point of origin (“vertex”)

Note: these lectures will not cover historical detector designs that are no longer in use.

The “ancestor” – and still in use: **Wire chambers**

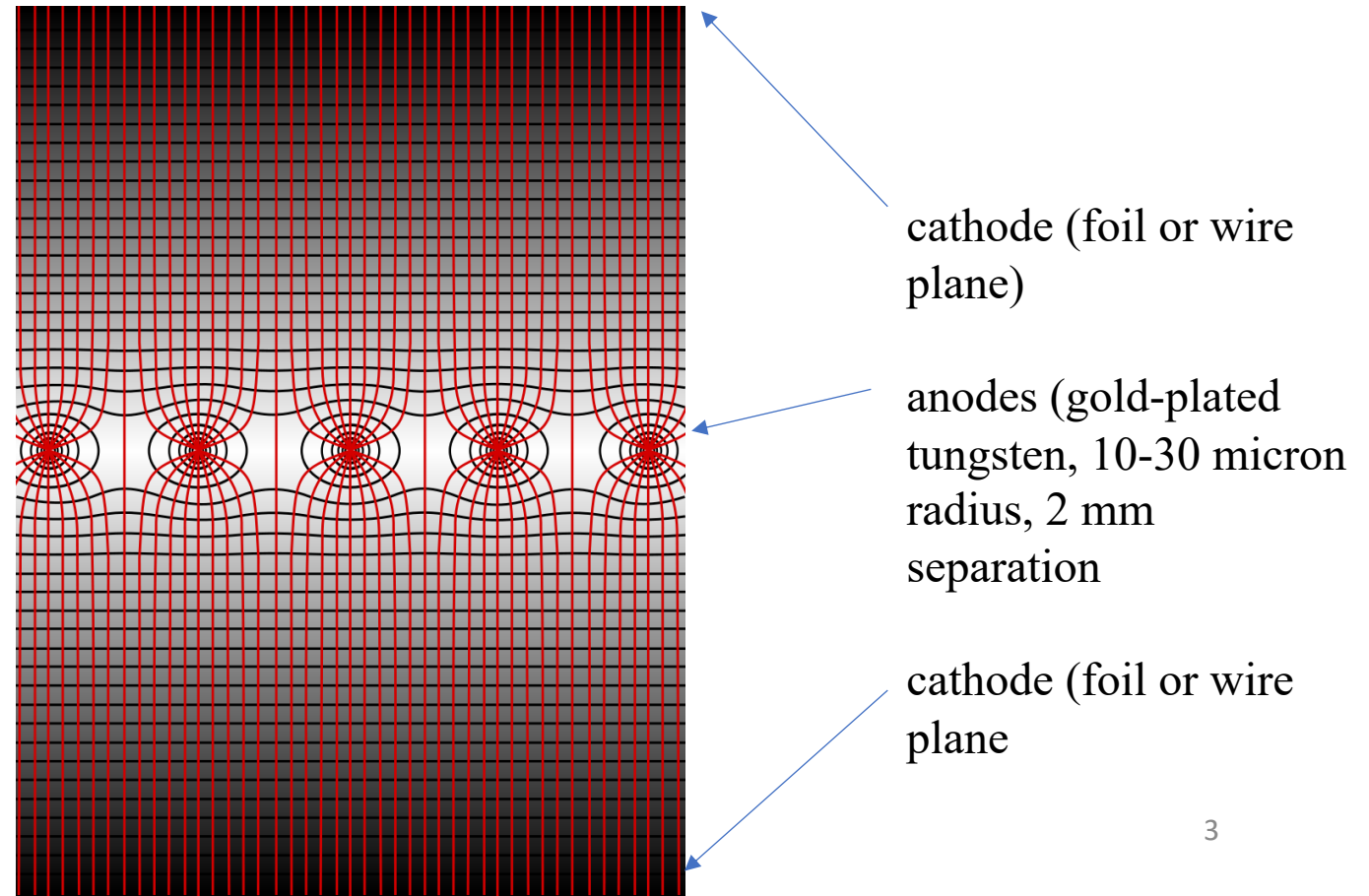
The single wire proportional counter: invented* by Geiger and Rutherford in 1908.

Multiwire proportional chambers (MWPC) were invented** by Georges Charpak in 1968 (Nobel Prize 1992)

MWPC: A planar layer of proportional counters without separating walls

produces field lines (red) and equipotential lines (black) like this:

- A through-going charged particle ionizes gas, produces primary electrons and ions along the track
- Primary electron drifting toward anode is accelerated by the E field, starts avalanche (ions + more electrons)
- Avalanche multiplication ends when positive ion space charge reduces E field below critical value
- Electron cloud drifts toward anode, ion cloud drifts (more slowly) to cathode.



* H. Geiger and E. Rutherford, Proc. Royal Soc. A 81:141 (1908).

** G. Charpak et al., Nucl. Instr. Meth. A 62: 262 (1969).

MWPC design considerations:

Position resolution σ , in the direction perpendicular to the wires, for wire separation d :

$$\sigma = \frac{d}{\sqrt{12}} = 580 \text{ microns} \quad (\text{for } d = 2 \text{ mm})$$

The wire separation is limited by ***electrostatic repulsion*** of the long anodes. Counterbalance this with ***wire tension***.

For anode voltage V , length ℓ , capacitance per length C , tension T , permittivity ϵ_0 , ***the requirement for stability*** is:

$$T \geq \left(\frac{V \ell C}{d} \right)^2 \cdot \frac{1}{4\pi\epsilon_0}$$

Capacitance depends on anode separation d , anode wire radius r , and perpendicular distance L from anode to cathode:

$$C = \frac{4\pi\epsilon_0}{2 \left(\frac{\pi L}{d} - \ln \frac{2\pi r}{d} \right)}$$

An anode wire of mass m ***sags under gravity*** (this reduces the homogeneity of the E field) by an amount:

$$f = \frac{m \ell g}{8T}$$

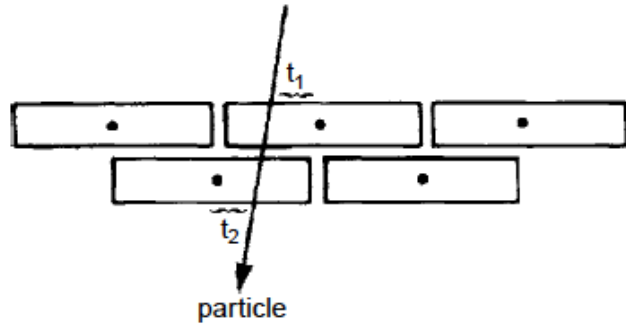
To improve spatial resolution in the direction along the wire:

-segment the cathode, then measure the charge induced on the cathode and calculate the center of gravity of the induced charge

- Resolution ~ 50 microns is typical for tracks perpendicular to the wire plane.

Using timing to improve the spatial resolution: **the drift chamber***

- Introduce potential wires between the anodes, to shape the drift field, *seeking well-mapped drift velocity v* .
- *Measure the time t* between particle traversal of chamber and electron cloud arrival at anode.

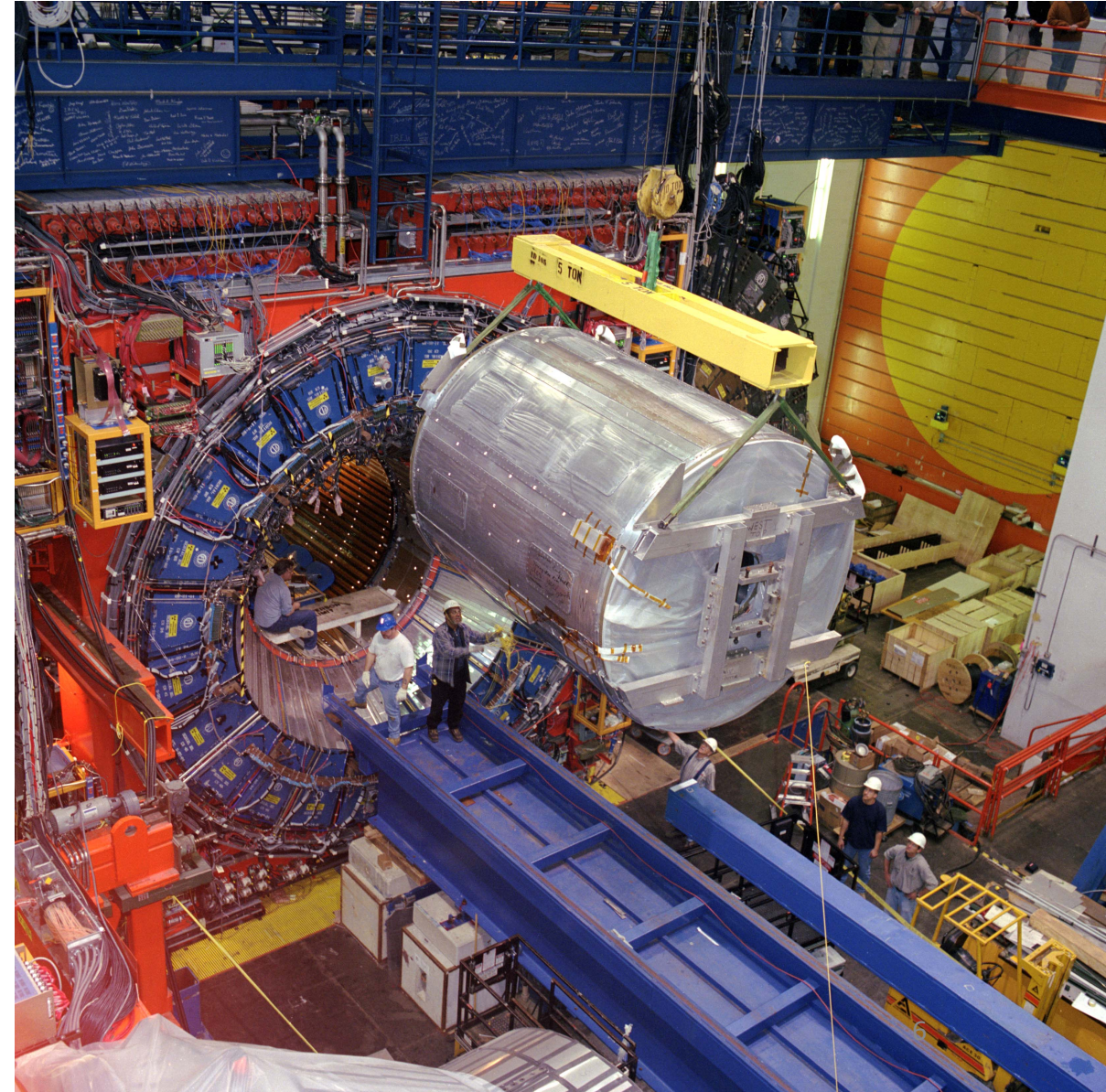


- *Perpendicular distance x from track to anode* is then

$$x = \int v^-(t) dt$$

- For electronic time resolution $\sim 1\text{ns}$, in smallish chambers not limited by mechanical tolerances, *spatial resolution on $\sigma_x \sim 20\mu\text{m}$* (ignoring fluctuations in formation of the primary ionization, and diffusion of the cloud).

Drift chambers can be big!
Installation of the the CDF Central Outer Tracker (drift chamber):



* A.H. Walenta et al., Nucl. Instr. Meth. A 92: 373 (1971).

Varieties of modern wire chambers

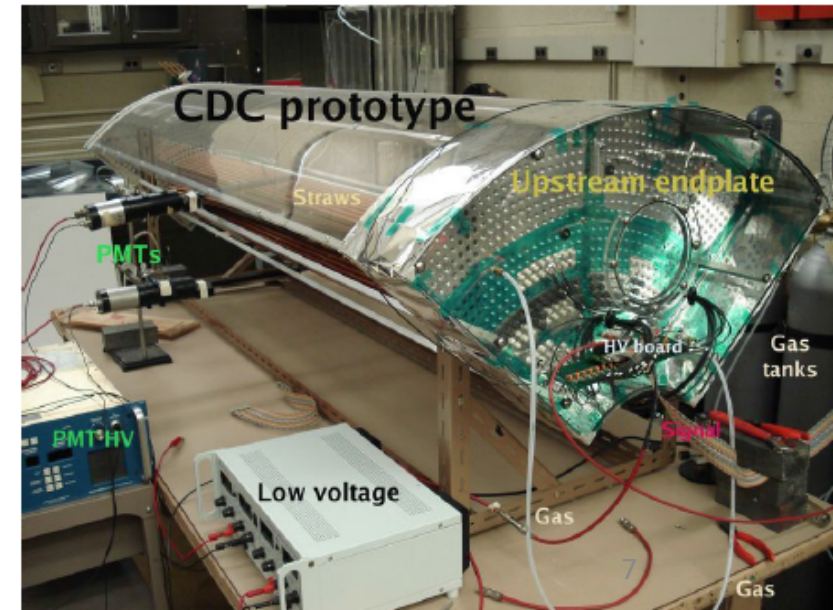
1) *Cylindrical proportional and drift chambers*

- Wires run axially, form cylindrical volumes
- Wires are stretched between 2 end plates, for total tension of tons
- Embed the chamber in an axial magnetic (B) field.
- Potential wire between each pair of anodes.
- Then these record track curvature to infer momentum p . For radius of curvature ρ ,

$$p[\text{GeV} / c] = 0.3B[\text{T}] \cdot \rho[\text{m}]$$

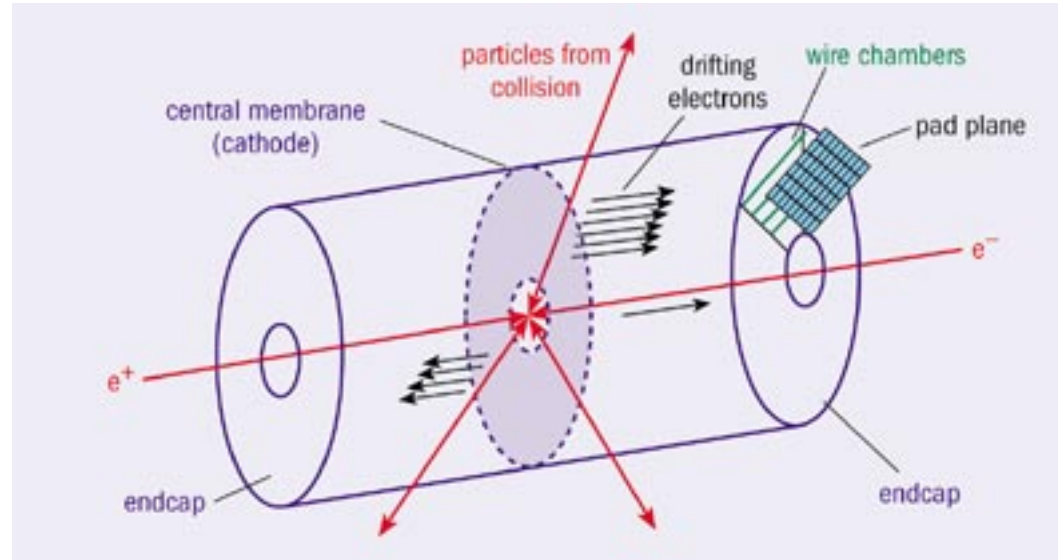
- To obtain axial position information: half of the anode wires are oriented at a small ***stereo angle*** ($\sim 2^\circ$) with respect to the z-axis.
- Drift cells can be “***open***” or “***closed***” depending on whether or not there is a field wire between every pair of anodes. Closed: shapes the field better, but costs more wires.
- *If a wire breaks* – a region of the chamber is disabled. To minimize this effect, ***surround each wire with a mylar foil (this is a “straw tube”)*** and the full assembly is a “straw chamber”

**$\frac{1}{4}$ prototype of the
GlueX straw
chamber**



2) **Time projection chambers*** (David Nygren, 1974) measure a 3-dimensional space point for every cluster of primary electrons, with *minimal multiple scattering*

- one central electrode
- E and B fields both axial (no $\mathbf{E} \times \mathbf{B}$ effect): charge drifts parallel to field lines.
- volume contains counting medium (gas or liquid) but no other components: minimal multiple scattering
- end plates are wire chambers



- Axial B field: suppresses perpendicular diffusion (charged particles spiral around the field lines)
- Arrival time of charge – determines the z coordinate of the event
- Anode wires in the endcaps – stretched in the azimuthal direction to measure radius r
- Cathode pads around the circumference of the end plates: to measure angle ϕ and radius r
- Analog signals on the anodes measure energy loss: particle ID

* D. Nygren et al., PEP-PROPOSAL-004, App. A6 (1976).⁸

Modern TPC's: can achieve very large volume. Detection rate is limited by drift + analog readout times; no amplification in noble liquids.

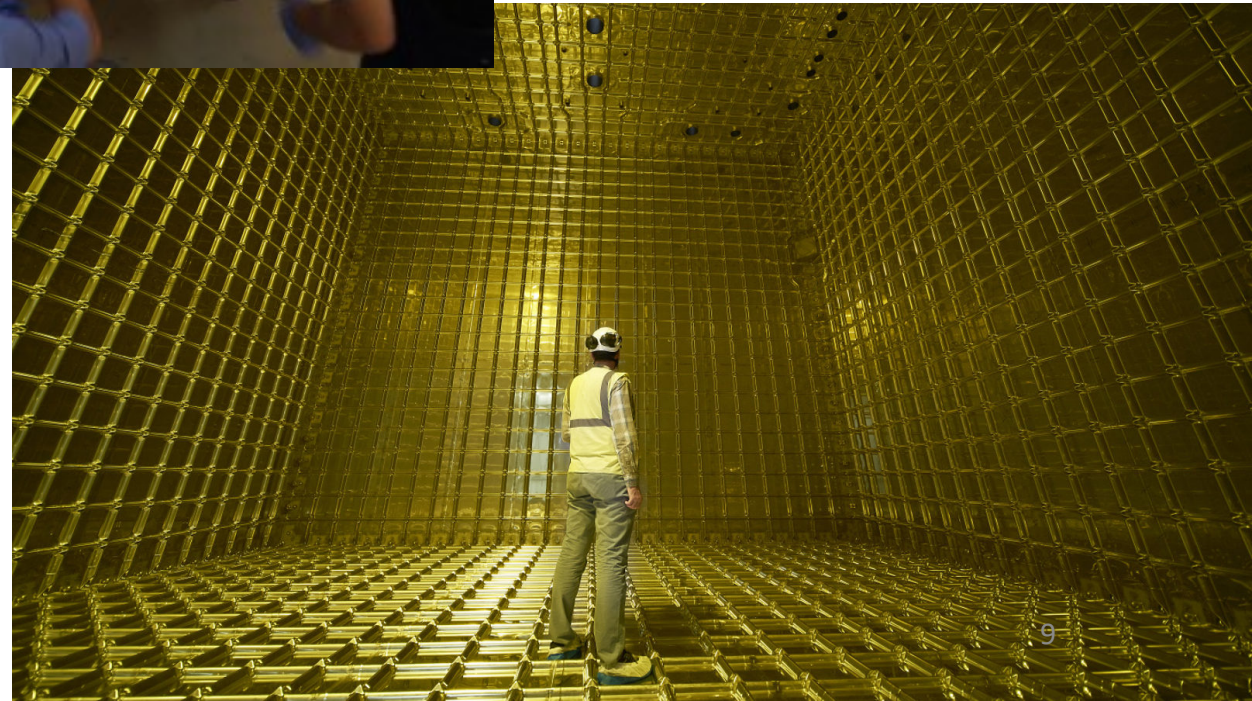


ALICE at CERN uses Ne-CO₂ gas



XENON dark matter experiment at Gran Sasso uses 62 kg dual phase (liquid/gas) Xe

Support structure for the liquid argon TPC (LArTPC) in DUNE



Improve resolution by *miniaturizing the ionization volume*: **Micro-pattern Gas Detectors**

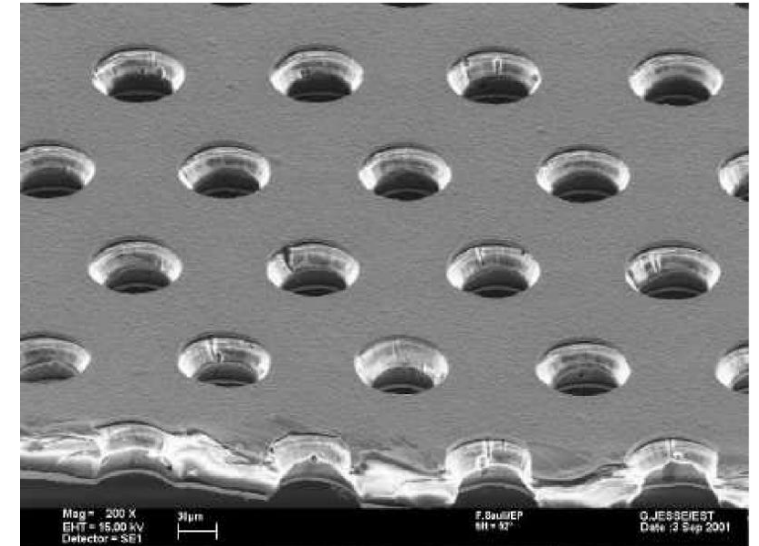
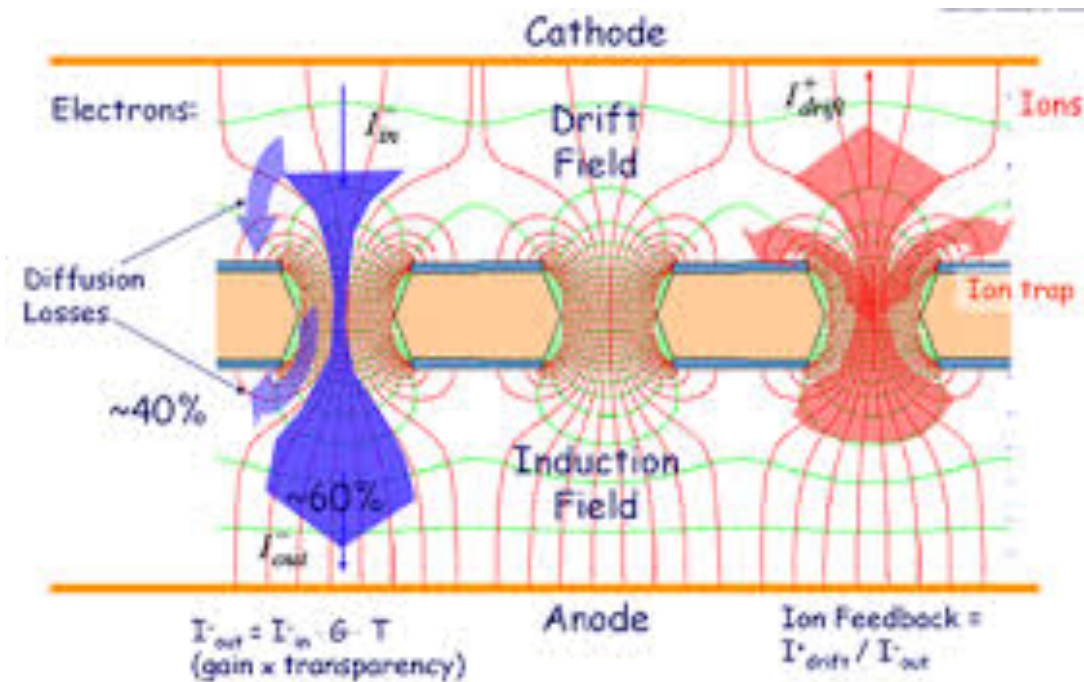
- These are MWPC's miniaturized (by \sim factor of 10), with gas gaps of $\sim 2 - 10$ mm.
- *Electrodes are formed by lithography on insulator or semiconductor surfaces* (i.e., no wires). Pitch $\sim 100 - 200$ microns.
- Strips or pixels
- *Low dead time* (ion drift distance to cathode is short).
- Many varieties, to *optimize against aging and for different conditions*.
- Examples (these both include an amplification structure): **Micromegas** and **GEM**

Improvement in rate capability: capable of $\sim 10^6$ Hz/mm²

Improvement in granularity: capable of ~ 30 μ m spatial resolution

Gas electron multiplier (GEM)*

Also include *a conversion gap*, plus *a multiplication region* produced by a thin insulating Kapton foil coated with metal film on both sides, and containing $\sim 50\text{ }\mu\text{m}$ holes on a $\sim 100\text{ }\mu\text{m}$ pitch. Different potentials on the films produce charge multiplication in the holes. **Gain** $\sim 10^5$ on electrons for cascaded arrays. Short gap restricts breakdown.

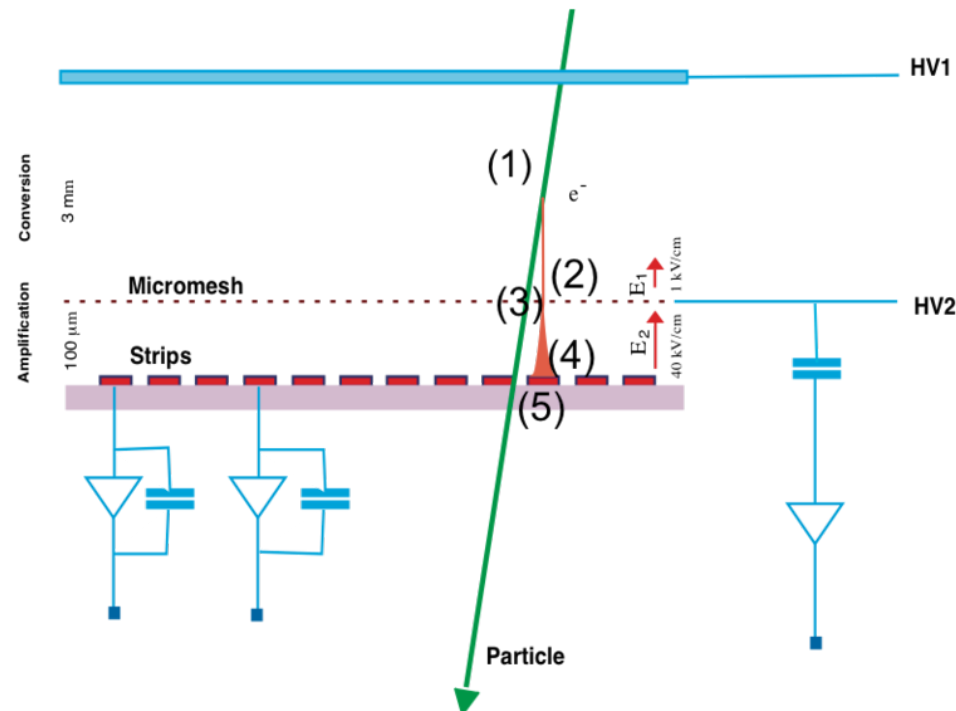


GEM technology is also proposed for the ILC TPC.

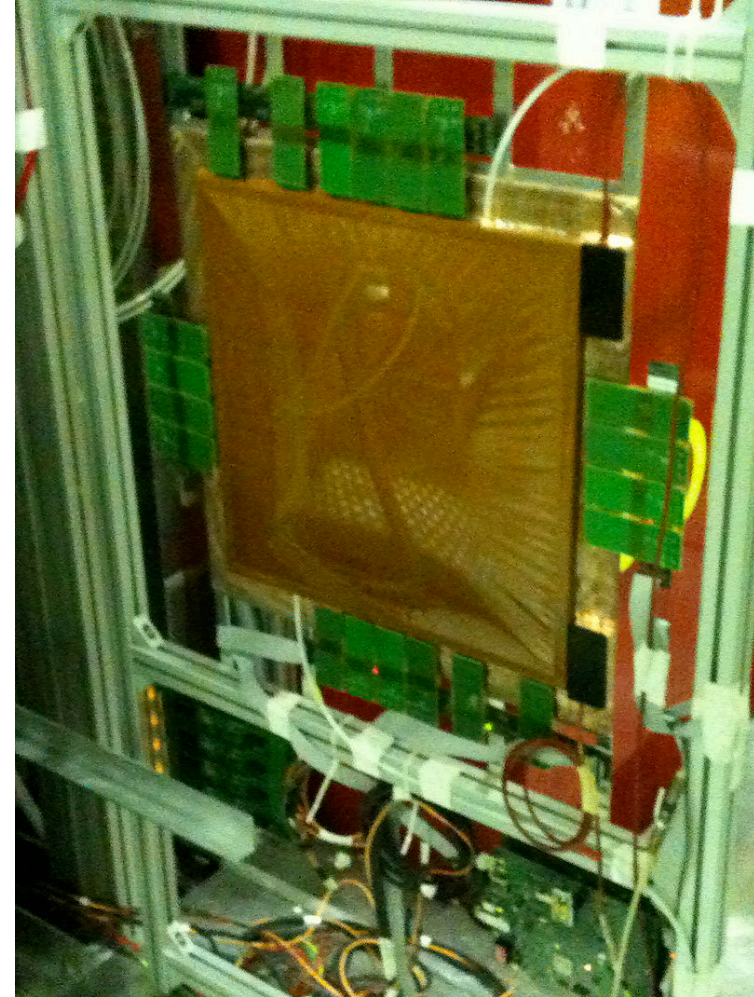
* F. Sauli, Nucl. Instr. Meth. A A 386: 531 (1997)

Micro-Mesh Gas Structure (Micromegas)*

- Primary electrons are produced in the ionization process in a **2-5mm conversion gap**, then drift to a **50-100 μm multiplication gap**, bordered by a cathode mesh and anode readout structure.
- High E field ($\sim 100 \text{ kV/cm}$) in the multiplication gap provides **gain $\sim 10^5$** on electrons.
- Ions are collected in the near cathode, so **timing precision and rate capability are good**.



Micromegas is operating in the COMPASS Experiment...



...and has been proposed for a “Micromegas TPC” at the International Linear Collider (ILC)

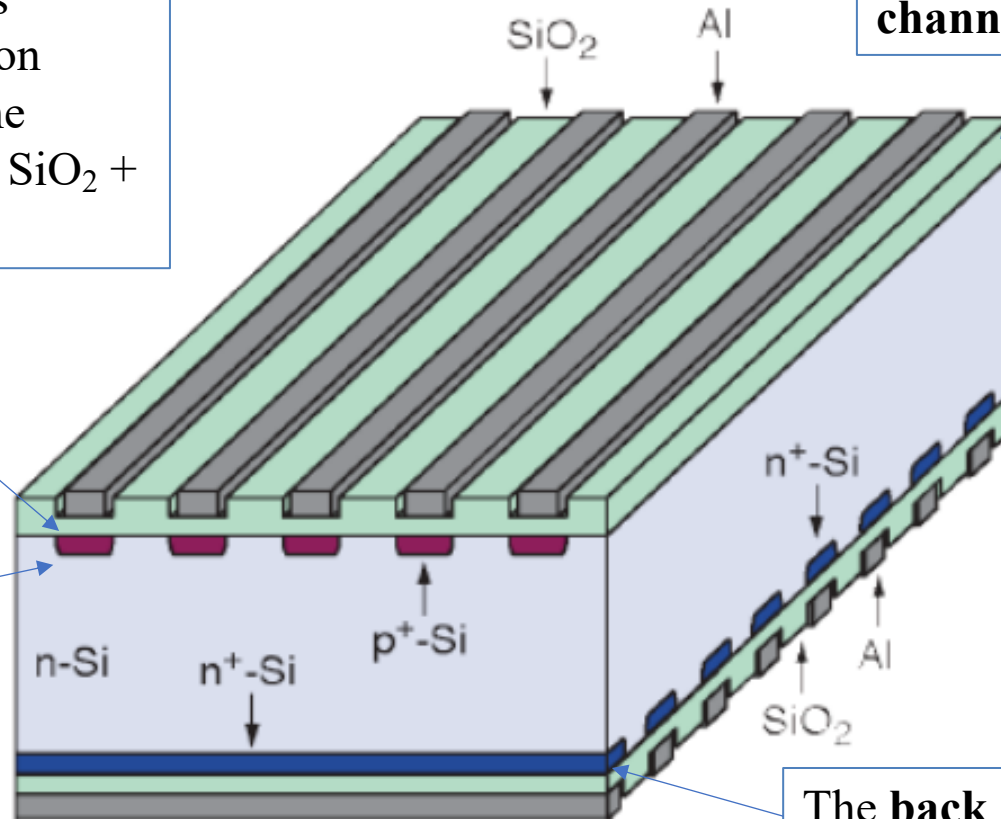
* Y. Giomataris et al., Nucl. Instr. and Meth. A 376: 29 (1996).

Silicon Pixel and Strip Detectors: replace the ionization medium (gas) with semiconductor, for the ultimate precision

In modern detectors, typically signal routed to read-out electronics is capacitively induced on **metal electrodes**. The capacitor dielectric is $\text{SiO}_2 + \text{Si}_3\text{N}_4$.

SiO_2 grows naturally on wafer surface, and electrically **isolates channels**.

The pn junction is at the interface of the bulk with these **implanted strips** (“p⁺” means $10^{18} \geq n_{\text{dopant}}/\text{cm}^3 \gg 10^{13}$). Under *reverse bias*, the region depleted of free carriers grows from the junction toward the n⁺ side (“back side”).



The **back side also takes an implant**, which can be segmented (in “double sided detectors”) or not.

Calorimetry: Measurement of Energy, Missing Energy, and Particle ID

Calorimetric method: *total absorption of the energy* of a particle, in material bulk, then measurement of the deposited energy. The particle is destroyed in the process.

Applies to *neutral and charged* particles.

Role of the calorimeter:

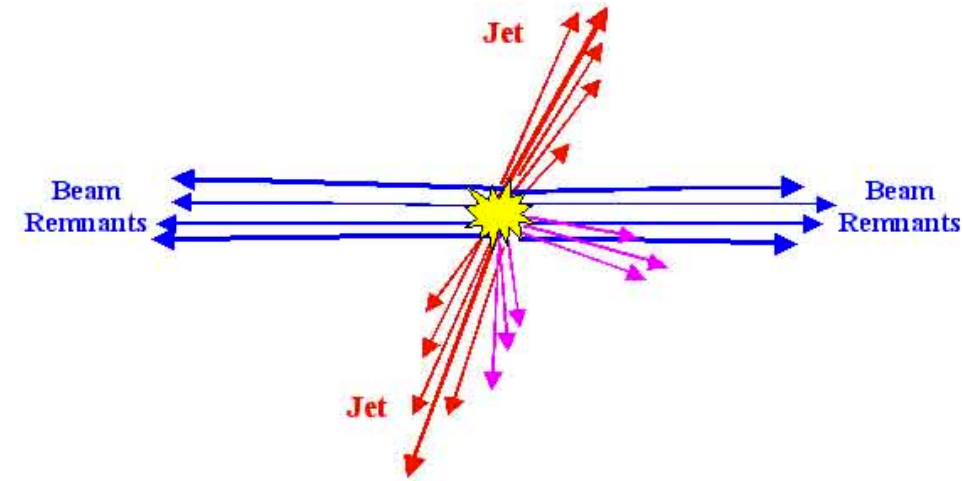
- precision measurement of the four-vectors of individual particles and jets
- measurement of mass peaks
- measurement of energy flow, to recognize missing energy
- identification of jet substructure
- rejection of pileup (multiple overlapping interactions during a single beam crossing)

Measurement principles use

- atomic and molecular excitation (ionization, scintillation)
- collective effects in the medium (Cherenkov light, phonons)
- heat deposition (transition from superconducting to normal)

In addition to measuring energy, *the calorimeter can provide full information on the track 4-vector as well as fast input to a detector trigger.*

Very different physics for detection of electromagnetically showering particles (electrons, positrons, photons) versus strongly interacting (i.e. hadronic) particles (pions, kaons, protons, neutrons)



Electromagnetic calorimetry

Principle of detection: Energy loss (dE/dx). Here is what dominates the process:

- for showering particles with energy $\sim \text{MeV}$
 - for photons - photoelectric and Compton
 - for charged particles – ionization and excitation
 - for showering particles with energy $\gtrsim 100 \text{ MeV}$
 - for photons – pair production
 - for charged particles – bremsstrahlung
- } These do not produce a shower / avalanche
- } These DO produce a shower / avalanche

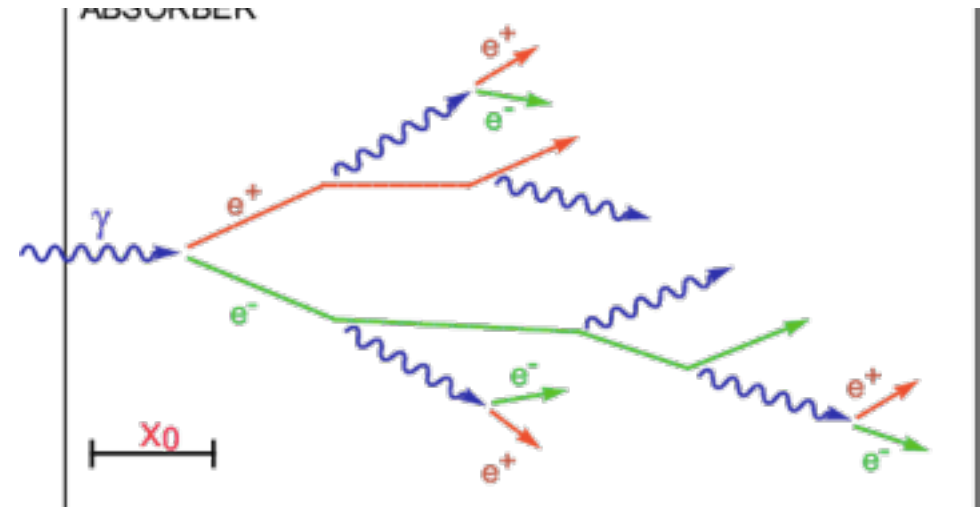
Recall that **radiation length X_0** characterizes the loss rate:

$$-\frac{dE}{dx} = \frac{E}{X_0}$$

Think of X_0 as “the typical distance the electron travels before it brems, or the typical distance the photon travels before it converts to a pair.”

Typically the **depth t** of an EM calorimeter is indicated in units of radiation lengths:

$$t = \frac{x}{X_0}$$



In a simplified model of the shower, *the # shower particles at depth t* is:

$$N(t) = 2^t$$

If the primary incident particle has energy E_0 , the *energy of each particle in generation t* is:

$$E(t) = E_0 2^{-t}$$

The *shower stops when*

$$E_0 / N < E_c$$

where E_c is a critical energy at which Compton/photoelectric/ionization begin to dominate (depends on the material).

Thus:

$$E_c = E_0 2^{-t_{\max}}$$

And the *position of the shower maximum* is

$$t_{\max} = \frac{\ln(E_0 / E_c)}{\ln 2}$$

Thus: in designing, **the thickness of the calorimeter should go as $\ln E_0$.**

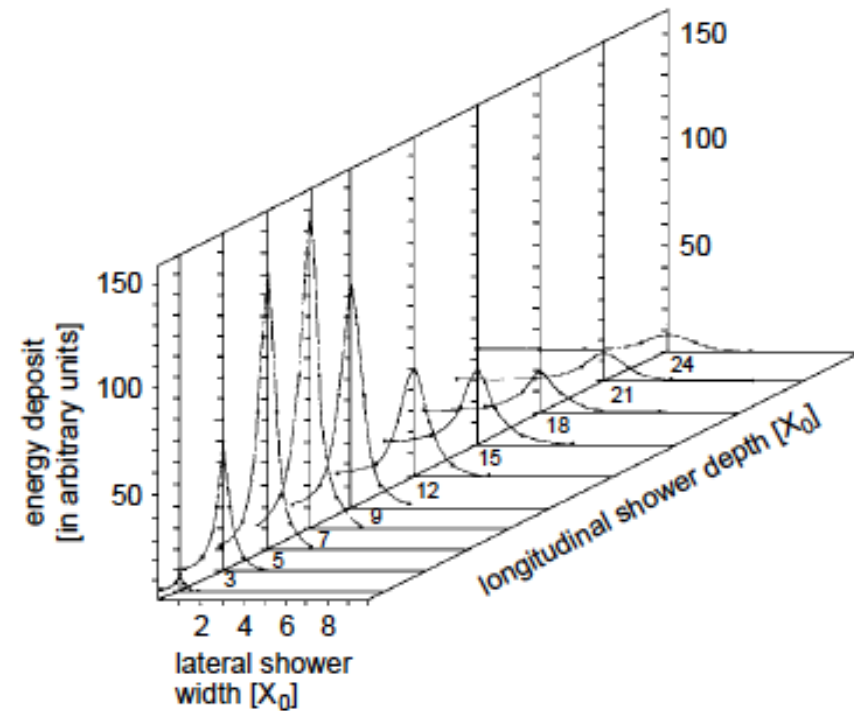
Note: below E_c , production of electrons and positrons stops within 1 X_0 , but photons continue to penetrate a further 7-9 X_0 . **To fully contain a shower, the calorimeter should have depth $\sim 16 X_0$.**

The actual formation of the shower is more complicated than this but can be well modeled using Monte Carlo, as:

$$\frac{dE}{dt} = E_0 \cdot b \cdot \frac{(bt)^{a-1} e^{-bt}}{\Gamma(a)}$$

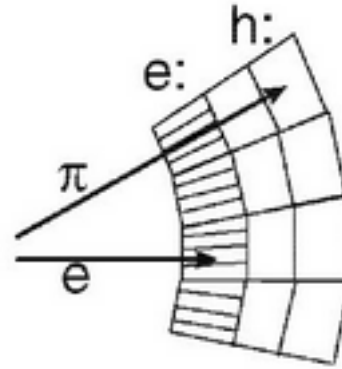
where

$$\Gamma(g) = \int_0^{\infty} e^{-x} x^{g-1} dx$$



(In dense media, the development of the shower is modified by the Landau-Pomeranchuk-Migdal (LPM) effect, a quantum mechanical effect which suppresses production of low energy photons. This must be considered at modern experiments such as those at the LHC.)

The **cascade is narrow** (Opening angle $\langle\theta^2\rangle \sim \gamma^2$ due to brem and pairs, and **increases** with depth due to multiple scattering of electrons, $\langle\theta\rangle \sim 1/E_e$.) Because showers broaden as they develop, calorimeters use projective geometry:



About **95% of a shower is contained within a cylinder about the axis, of radius $2R_M$** , where

$$R_M = \frac{21 \text{ MeV}}{E_c} X_0 [\text{g/cm}^2] \quad \text{is the Moliere radius.}$$

The **resolution of a calorimeter is approximately equal to the non-containment fraction**. Thus 5% non-containment translates to about 5% resolution.

The shower profiles have long tails: increasing the collection from 90% to 99% requires an order of magnitude more mass.

The energy deposited in the medium is due to the ionization losses of the charged particles \propto # of electrons and positrons.

To detect this energy, 2 processes are needed:

- 1) The energy is transferred from the particle to the medium – *“the particle is absorbed”*
- 2) *The energy is read out* - detected

Two options for EM calorimeter configuration:

- *homogeneous*: the absorber and the detector are combined
- *sampling*: the absorber and the detector are distinct

Homogeneous calorimeters – the full volume of the detector can absorb the energy and transmit it to readout

Measurement principle is any of these:

- detection of *scintillation* light (medium is scintillating crystals or liquid noble gas)
- collection of *ionization* (medium is liquid noble gas)
- generation of *Cherenkov* light (medium is heavy transparent crystal or lead glass)

The most important features of the calorimeter are the position and energy resolutions for photons and electrons.

Energy resolution:

$$\frac{\sigma_E}{E} = \frac{a}{\sqrt{E}} \oplus \frac{b}{E} \oplus c$$

crystal non-uniformity ($c < 1\%$)
electronics noise ($b \sim 100$'s of MeV)
photoelectron statistics ($a \sim 3\%-5\%$)

Notice: the resolution improves with increasing energy.

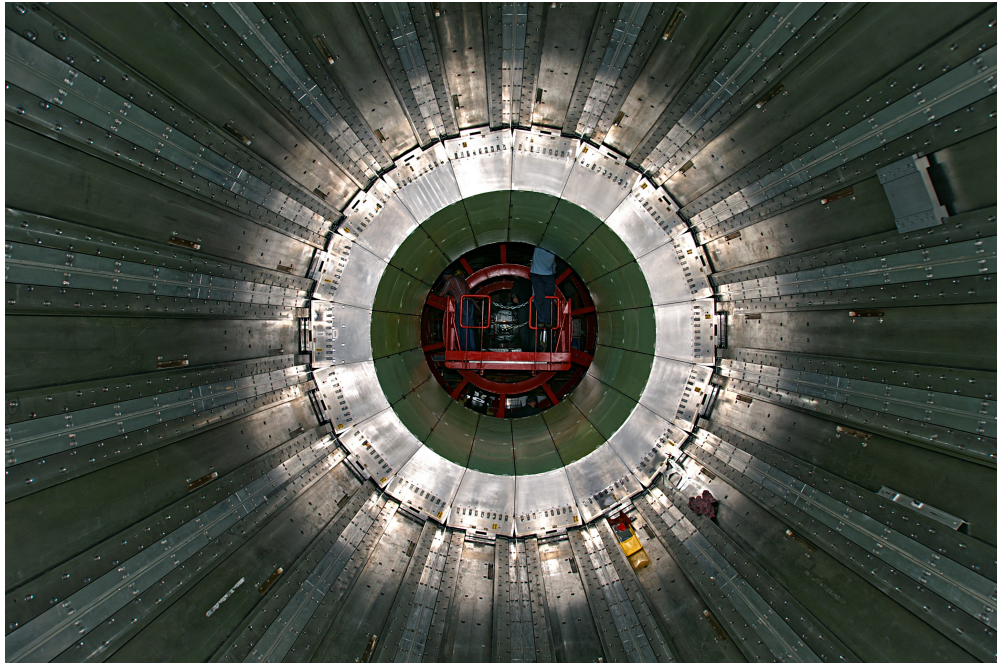


Example homogeneous calorimeter types:

1) **Crystal** calorimeters -best resolution at this time: $\sigma_E/E \sim 1\%$

(Lead glass calorimeters – less expensive than crystals, but lower Cherenkov light production increases resolution to $\sim 5\%/\sqrt{E}$)

2) **Ionization** calorimeters – often using noble liquids: liquid argon (LAr) is abundant, inexpensive, obtainable with high purity, radiation hard



ATLAS LAr EM Calorimeter
(ionization principle)

CMS Ecal: 80k PbWO_4 (lead tungstate) *crystals*, mounted inside 4T solenoid: **Strengths:** short radiation length, small Moliere radius, fast scintillation emission, high radiation hardness. **Challenge:** low light output.

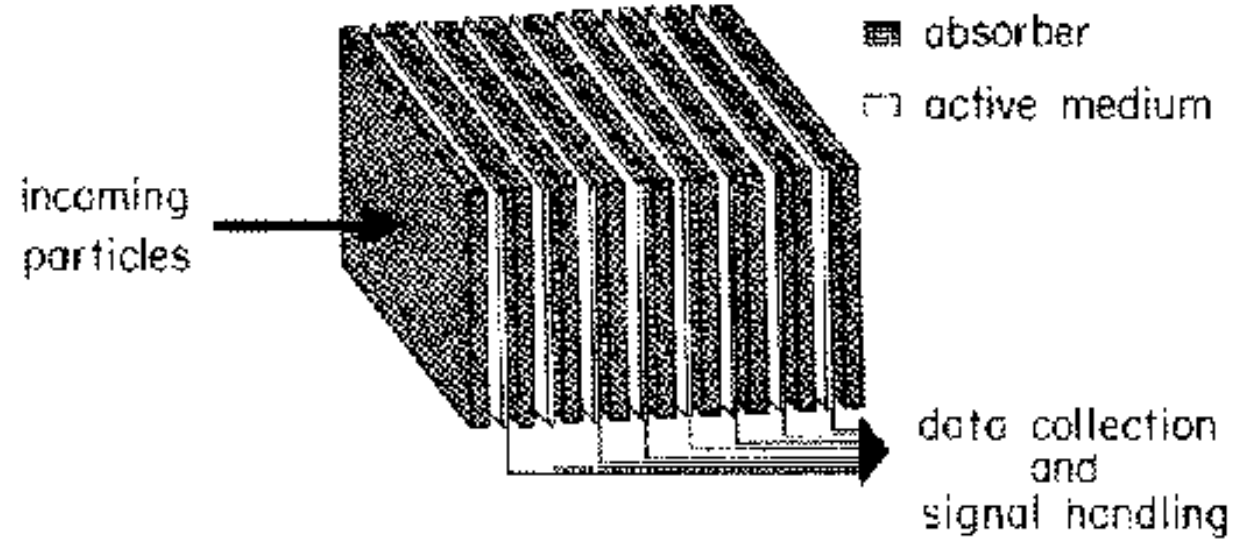


Calorimeter position resolution is taken from the corrected center of gravity of the energy deposition. Approximately,

$$\sigma_{longitudinal-position} \sim \frac{R_M}{\sqrt{E / E_c}} \sim \text{few mm for } E_\gamma = 1 \text{ GeV with crystals}$$
$$\sigma(\theta) \sim \frac{\text{few mrad}}{\sqrt{E}}$$

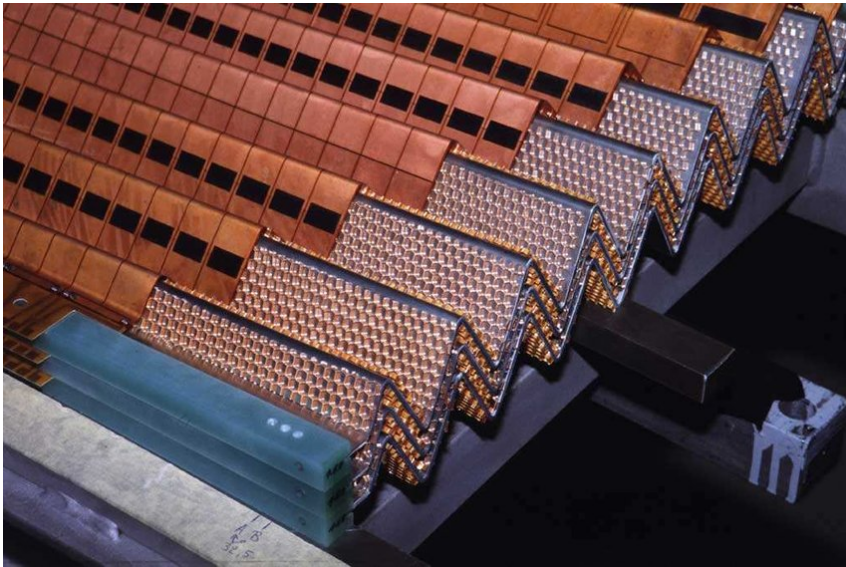
Sampling calorimeters – longitudinal stack of absorbers separated by thin counters

- **Typical sensors:** gas-filled ionization chambers, cryogenic noble gases (LAr, LXe) as ionization chambers, warm liquids, scintillators
- **Typical absorbers:** U, Fe, W, Cu, should be > 2 cm thick
- **Advantage:** each material can be separately optimized
- **Disadvantage:** contribution to resolution from sampling fluctuations (minimized in dense materials: typically $\sim 8\%$ in LAr @ 1 GeV).



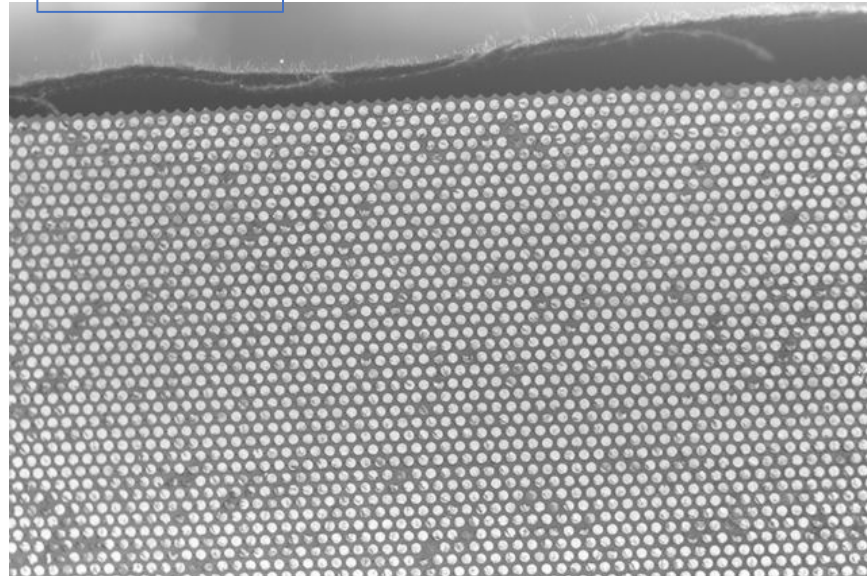
Sampling calorimeters, continued

Layers can be planes, or more complicated. To avoid “cracks” (gaps between adjacent towers): see the *accordion* chamber...



...and the *spaghetti* calorimeter, in which the counters are fibers embedded in the absorber...

KLOE Exp.



...and more geometries: shashlik-calorimeter, tile-calorimeter....

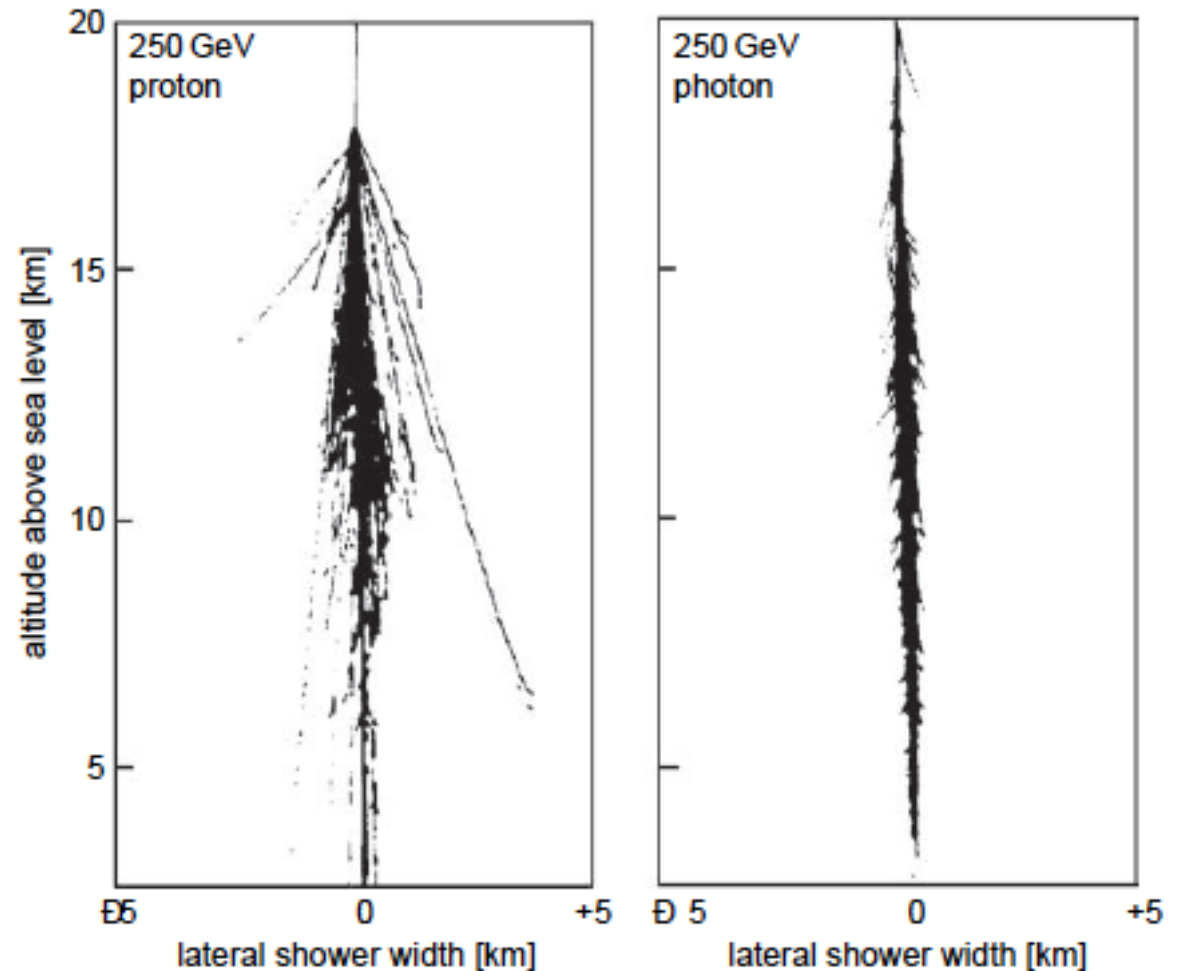
Hadronic calorimetry – to measure the energy of non-showering particles

- Similar geometries, but the *longitudinal shower development is determined by nuclear interactions*
- Showers include pions, kaons, nucleons
- Characterized by the *nuclear interaction length*:

$$\lambda_I \sim 35 \left[\frac{g}{\text{cm}^2} \right] A^{1/3}$$

This is longer than X_0 for most materials.

- Hadronic showers are broader than EM showers due to large transverse momentum transfers in nuclear interactions. Compare simulated air showers of equal-energy proton and photon.



How is the hadron energy dissipated in the absorber?

- 1/3 of the hadrons produced are π^0 . These decay quickly to photons, producing EM showers.
- Another 30%-40% of the hadron energy is dissipated invisibly as **broken nuclear bonds or production of stable neutrals** (neutrons, K_L^0).
- ***ONLY the EM energy dissipated by charged particles is recorded by any calorimeter***, so the hadron signal is smaller than the EM calorimeter signal, for the same particle energy. *Up to 40% of the non-EM energy may be “invisible”* – binding energy of nucleons released in nuclear reactions – with large event-to-event fluctuations.
- Large fluctuations in hadron shower development (i.e. fluctuations in number of π^0 's) leads to *worse resolution than in EM calorimeter*
- *Hadron calorimeters are intrinsically nonlinear with energy* – the average EM fraction (called “e”) increases with energy.
- The response of the calorimeter to the non-EM fraction (called “h”) is constant with energy. Thus:

$$\frac{e}{h} > 1$$

“**Compensation**” is a technique to recover information on the invisible energy, i.e. to achieve $\frac{e}{h} \rightarrow 1$

Only sampling calorimeters can be compensated.

Compensation methods:

- *suppress the EM response* (e.g. choose high-Z absorber material)
- *boost the non-EM response* (choose an absorber containing hydrogen; incoming neutrons recoil on the protons, which then contribute to the signal)
- “*offline compensation*” – determine the energy sharing between EM and hadronic components on an event-by-event basis through analysis of event characteristics (shower shape, composition) – this is “Dual REadout Method” (DREAM) calorimetry.
- uranium absorber – *fission materials liberate additional energy*

ZEUS (uranium/scintillator) achieved $\frac{\sigma}{E} \sim \frac{35\%}{\sqrt{E}}$. ATLAS (non-compensating) “Tile” calorimeter achieves $\frac{\sigma}{E} \sim \frac{42\%}{\sqrt{E}}$

Calorimetry applications outside the realm of particle accelerators:

- energy measurements of *extensive cosmic ray showers induced in the atmosphere*: detect scintillation or Cherenkov light (Pierre Auger, HiRes Fly's Eye).
- energy measurements of cosmic neutrinos or muons: “*neutrino telescopes*” employing photo detectors in a matrix of absorber deep underground or in the sea (Kamiokande, IceCube, SNO).
- detection of *extremely low energy particles* (e.g. hypothesized WIMPs). This requires cryogenic operation to suppress thermal noise.

Phonons provide a signal in the μeV to meV range, detectable with classical calorimetry via energy deposition in an absorber (CRESST detectors, CYGNUS, DRIFT)

